

EAGLE: Elevating Geometric Reasoning through LLM-empowered Visual Instruction Tuning

Zhihao Li^{1*}, Yao Du^{1,2†}, Yang Liu¹, Yan Zhang³, Yufang Liu^{1,4}, Mengdi Zhang¹, Xunliang Cai¹

¹Meituan, Beijing, China

²Beihang University, Beijing, China

³Tianjin University, Tianjin, China

⁴East China Normal University, Shanghai, China

{zhihao.lics, yfliu.antnlp}@gmail.com, duyao@buaa.edu.cn, yzhang1995@tju.edu.cn, {liuyang509, zhangmengdi02, caixunliang}@meituan.com

Abstract

Multi-modal Large Language Models (MLLMs) have recently experienced rapid developments and excel in various multi-modal tasks. However, they still struggle with mathematical geometric problem solving, which requires exceptional visual perception proficiency. Existing MLLMs mostly optimize the Large Language Model (LLM) backbone to acquire geometric reasoning capabilities, while rarely emphasizing improvements in visual comprehension to better distinguish geometric elements. In this paper, we first investigate the visual perception performance of MLLMs when facing geometric diagrams. Our findings reveal that current MLLMs severely suffer from inaccurate geometric perception and hallucinations, which hinders their performance in solving geometric problems. To address these limitations, we propose **EAGLE**, a novel two-stage end-to-end visual enhancement MLLM framework designed to Elevate Geometric reasoning through LLM-Empowered visual instruction tuning. Specifically, in the first preliminary stage, we feed geometric image-caption pairs into our MLLM that contains a fully fine-tuning CLIP ViT and a frozen LLM, aiming to endow our model with basic geometric knowledge. In the subsequent advanced stage, we incorporate LoRA modules into the vision encoder and unfreeze the LLM backbone. This enables the model to leverage the inherent chain-of-thought (CoT) rationales within question-answer pairs, guiding the MLLM to focus on nuanced visual cues and enhancing its overall perceptual capacity. Moreover, we optimize the cross-modal projector in both stages to foster adaptive visual-linguistic alignments. After the two-stage visual enhancement, we develop the geometry expert model EAGLE-7B, which holds exceptional proficiency in geometric problem solving. Extensive quantitative and qualitative experiments on popular benchmarks demonstrate the effectiveness of our model. For example, on the GeoQA benchmark, EAGLE-7B not only surpasses the exemplary G-LLaVA 7B model by 2.9%, but also marginally outperforms the larger G-LLaVA 13B model. On the MathVista benchmark, EAGLE-7B achieves remarkable 3.8% improvements compared with the proprietary model GPT-4V. Our code and model will be released soon.

*This work was done during his internship at Meituan.

†Corresponding author.

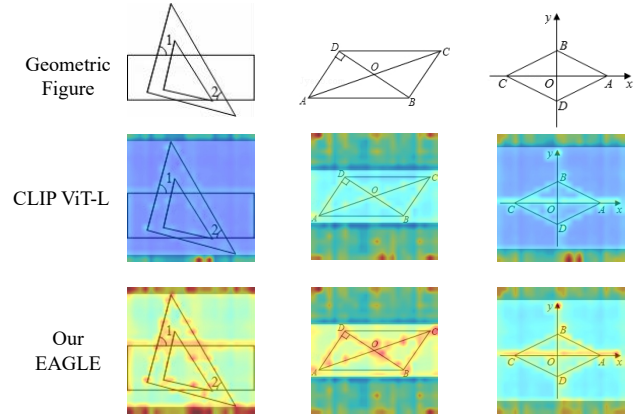


Figure 1: Comparison of attention maps between CLIP ViT (Radford et al. 2021) and our EAGLE. We utilize the attention rollout technique (Abnar and Zuidema 2020) for visualization. It is clear that EAGLE displays superior proficiency in capturing key geometric elements.

Introduction

Large Language Models (LLMs) have undergone flourishing developments and demonstrated remarkable performance across a variety of tasks. Latest LLMs even exhibit human-level reasoning capabilities in complicated tasks such as mathematical problem solving (Imani, Du, and Shrivastava 2023) and code generation (Chai et al. 2024; Sun et al. 2024). However, these studies mainly focus on mathematical reasoning in textual contexts, while multi-modal mathematical problems (e.g., geometric problems) are also vital in practice and require the model to have visual comprehension proficiency. Since LLMs lack the capability to “see”, they inevitably face a performance ceiling. Consequently, Multi-modal Large Language Models (MLLMs), which extend LLMs by incorporating an extra vision encoder, have attracted substantial research attention.

Early MLLM studies mainly concentrate on general multi-modal tasks, such as image caption (Xu et al. 2015), visual question answering (Antol et al. 2015), and image retrieval (Ji et al. 2024). As a milestone work, LLaVA (Liu

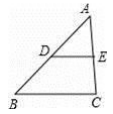
et al. 2024b) successfully integrates a vision encoder with the LLM backbone, developing a highly capable instruction-following visual agent. However, compared with proprietary MLLMs such as GPT-4V (OpenAI 2023), general open-source MLLMs still fall short in solving mathematical problems in visual contexts, especially for geometric problems. Recently, several works (Gao et al. 2023; Shi et al. 2024) proposed to inject geometric knowledge into MLLMs with extensive geometric question-answer examples. Despite their progresses, these studies mainly focus on improving the reasoning capacity of the inherent LLM backbone, while rarely exploring the reliability of MLLMs’ visual comprehension, which is typically facilitated by the versatile CLIP ViT (Radford et al. 2021). However, due to the substantial domain gap between CLIP’s pre-trained data and mathematical geometric diagrams, CLIP’s visual perception proficiency in the specific geometric domain is questionable. In light of this proposition, we make attempts to examine the perception performance of CLIP and explore the geometric caption capability of MLLMs. As visualized in Figure 1 and Figure 2, the CLIP ViT falls short in effectively capturing geometric elements, such as points, lines, and angles. Moreover, we observe that existing MLLMs suffer from severe geometric hallucinations and struggle to provide accurate geometric descriptions. These visual inadequacies compromise the perceptual precision of MLLMs built upon CLIP, subsequently impeding their performance in geometric problem solving.

To alleviate above limitations, we propose **EAGLE**, a novel two-stage end-to-end visual enhancement framework that progressively ElevAtes Geometric reasoning through LLM-Empowered visual instruction tuning. The core idea is to leverage powerful LLMs to promote the visual augmentation on specific geometric domains. We accomplish this design with a standard MLLM training framework, including a vision encoder, a cross-modal projector, and a LLM backbone. Specifically, EAGLE consists of two stages: preliminary visual enhancement with a frozen LLM and advanced visual enhancement with a dynamic LLM. In the first stage, we fine-tune the vision encoder with 60K geometric image-caption pairs while keeping the LLM backbone frozen, endowing our model with basic geometric knowledge. In the second stage, based on the acquired fundamental geometric intelligence, we incorporate LoRA modules to refine the vision encoder, which enables a deeper exploration of nuanced geometric details while preserving overall geometric comprehension. Meanwhile, we unfreeze the LLM backbone to promote the core geometric reasoning capability. With 110K chain-of-thought (CoT) based question-answer pairs, our model could distinguish delicate geometric clues that are critical for solving geometric problems, thus achieving deeper geometric comprehension. Moreover, we optimize the cross-modal projector at both stages to foster adaptive geometric visual-linguistic alignments. To summarize, our contributions are three-fold:

- **Observation on Inadequate Visual Perception Capability.** To investigate the geometric perception performance of existing MLLMs, we visualize the attention map of their vision encoder and explore their geometric

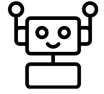


Please describe this geometric image in detail.



The image features a triangle with a square inside it, forming a unique shape. The triangle is composed of three sides, with one side being longer than the other two. The square is positioned within the triangle, with its corners meeting the triangle’s sides. The triangle is also accompanied by a smaller triangle, which is located at the top left corner of the main triangle. The image is presented in black and white, giving it a classic and elegant appearance.

LLaVA-1.5-7B



In the diagram, there is a triangle labeled ABC with vertices A, B, and C. A line DE is drawn parallel to the side BC of the triangle. Point D lies on the side AB, and point E lies on the side AC.

EAGLE-7B:



Figure 2: Illustration of the geometric caption performance of state-of-the-art MLLMs and our EAGLE. Captions with red background indicates visual hallucinations. EAGLE exhibits remarkable geometric perception capability after the preliminary visual enhancement, while the comparative model LLaVA-1.5 (Liu et al. 2024a) faces severe visual hallucinations.

caption capacity. We observe that the CLIP ViT adopted by MLLMs struggles to provide reliable visual comprehension, and current MLLMs suffer from severe geometric hallucinations. These deficiencies severely limit MLLMs’ performance in solving geometric problems.

- **Two-stage LLM-empowered Visual Enhancement Framework.** We propose a two-stage end-to-end LLM-empowered visual enhancement framework to improve MLLMs’ inadequate visual recognition capabilities. In the first preliminary stage, we fine-tune the vision encoder with a frozen LLM to endow our model with basic geometric knowledge. In the second advanced stage, we incorporate LoRA modules into the vision encoder and unfreeze the LLM backbone for more in-depth comprehension. Guided by the CoT rationales within the question-answer pairs, our model focus on more subtle details and achieve superior geometric problem-solving performance.
- **Mathematical Geometric Expert.** After the two-stage visual instruction tuning, we develop the geometric expert model EAGLE, and verify its effectiveness on two popular geometry benchmarks, namely GeoQA and MathVista. EAGLE achieves pioneering performance compared with leading MLLMs, and outperforms the representative G-LLaVA 13B model with only 7B parameters. Extensive quantitative and qualitative analyses further demonstrate the efficacy of our model.

Observation

Existing MLLMs mostly utilize a fixed CLIP ViT (Radford et al. 2021) as the vision encoder to comprehend visual diagrams, then perform reasoning with the base LLM backbone. Ensuring the feasibility of this paradigm relies

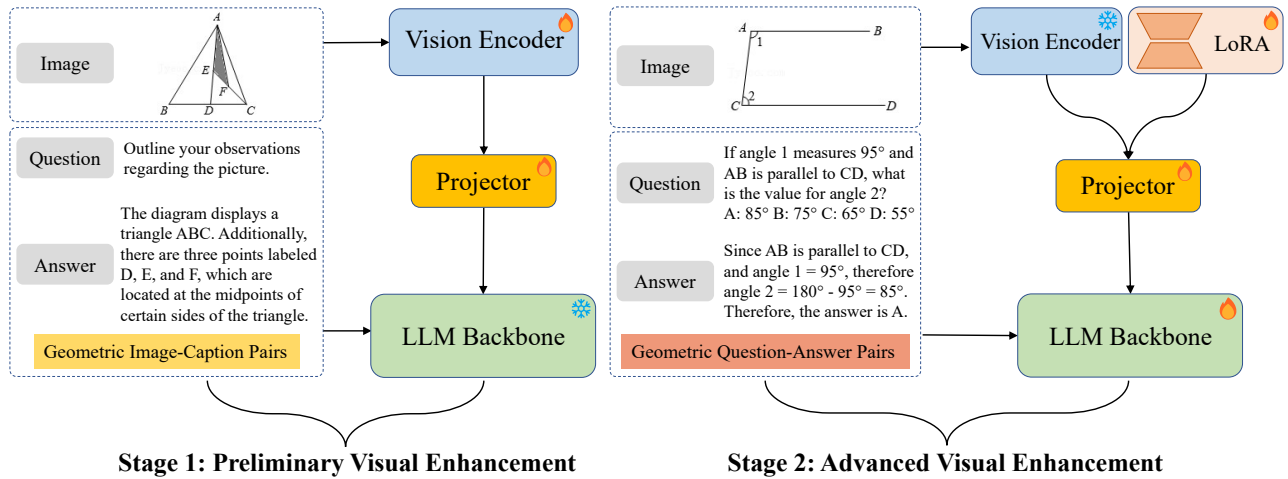


Figure 3: The overview of our proposed two-stage LLM-empowered visual enhancement framework. In the preliminary stage, we set the vision encoder and the projector to be trainable, while keeping the LLM backbone frozen, which aims at endowing the vision encoder with basic geometric perception proficiency. In the advanced stage, we integrate LoRA modules into the augmented vision encoder, and jointly fine-tune the projector and the LLM backbone. Guided by detailed CoT rationales, our model gradually focuses on nuanced geometric elements and acquires high-level geometric reasoning capability.

on maintaining the reliability of the vision encoder. However, due to the disparity between CLIP’s pre-trained natural images and specific mathematical diagrams, there is a high likelihood that CLIP may struggle to accurately capture specific geometric elements. Therefore, to investigate the geometric perception performance of current MLLMs, we visualize the attention map of CLIP ViT and examine the performance of MLLMs in generating captions with geometric contexts. Through this analysis, we observe two significant phenomena as follows:

- **Insufficient perception on visual clues.** As shown in Figure 1 and Appendix (1.A), CLIP struggles to effectively capture critical information within mathematical diagrams. Specifically, CLIP ViT-L fails to focus on general geometry elements (e.g., line, dot, angles) and corresponding marks (e.g., angle 1, vertex A). Such observation reveals that integrating a frozen vision encoder into MLLMs is inadequate to capture essential visual details for subsequent reasoning, which hinders the geometric problem-solving capability of MLLMs.
- **Severe visual geometric hallucinations.** Multi-modal hallucinations often entail the generation of descriptions for non-existent elements (Zhang et al. 2024a). Similarly, MLLMs also encounter these issues when processing geometric diagrams. As shown in Figure 2, they tend to generate non-existent objects or inaccurately describe the relative relationships among existing elements. These hallucinations result in unreliable geometric comprehension, greatly hindering the problem-solving capabilities. Therefore, this observation further demonstrates the necessity to enhance MLLMs’ vision encoder to ensure precise geometric comprehension.

Method

To mitigate the visual deficiency discovered in our previous observation and enhance geometric reasoning, this section introduces our proposed EAGLE in detail. The core idea involves leveraging the strength of LLMs to facilitate an geometric augmented vision encoder, which further leads to the geometric expert MLLM. To accomplish this aim, we devise a novel two-stage end-to-end visual enhancement framework to progressively endow MLLMs with geometric expertise, as depicted in Figure 3.

Stage 1: Preliminary Visual Enhancement with a Frozen LLM

As discussed in the Observation Section, MLLMs equipped with CLIP ViT exhibit severe visual shortcomings when recognizing geometric diagrams, which greatly hinders their performance in visual mathematics. To mitigate this issue, we propose to utilize 60K geometry image-caption pairs from Geo170K (Gao et al. 2023) to endow CLIP ViT with preliminary geometric knowledge. Concretely, we fully fine-tune a pre-trained CLIP ViT-L/14 model through the standard MLLM training scheme, where we employ a LLM as the cognitive core and a simple two-layer MLP as the cross-modal projector. Note that the CLIP ViT is integrated within an end-to-end MLLM framework, rather than being optimized independently and subsequently integrated as the vision encoder. In this scenario, we utilize the powerful LLM to encode the geometric captions, instead of relying on the original CLIP text encoder. This approach enables more precise and comprehensive linguistic understandings, thereby enhancing the performance of the geometry-augmented vision encoder. Moreover, we optimize the cross-modal projector to facilitate geometric vision-language alignments. To summarize, we freeze the LLM backbone and focus on train-

ing the vision encoder and the cross-modal projector during this stage.

Stage 2: Advanced Visual Enhancement with a Dynamic LLM

After the preliminary stage, abundant geometric diagram-caption pairs have equipped our MLLM with basic geometric cognition proficiency. To further exert LLM’s guidance role in solving geometric problems, we undertake an innovative attempt to optimize the vision encoder and the LLM backbone simultaneously, which is distinguished from existing geometric-focused MLLMs. Specifically, to guide the vision encoder to focus on subtle geometric details while preserving its acquired geometric knowledge, we incorporate LoRA (Hu et al. 2022) modules into the vision encoder and unfreeze the core LLM. Then, we utilize 110K multi-modal CoT question-answer pairs from Geo170K (Gao et al. 2023) to equip our model with solid geometric problem-solving capabilities. As the LLM backbone gains knowledge from the step-by-step rationales, the LoRA-based vision encoder gradually focuses on key geometric clues that are critical in the resolution process. This synergy further promotes an in-depth geometric comprehension. In this stage, we set the LoRA-based vision encoder, the cross-modal projector, and the LLM backbone to be trainable.

Model Training

In both the preliminary and advanced visual enhancement stages, we utilize a common auto-regressive language modeling loss. To generate the t^{th} token, we feed the geometry diagram I , the input sentence S_{in} , and the predicted tokens up to the t^{th} step into our model \mathcal{F} for next-token predictions. This process can be formulated as follows:

$$\mathcal{L}(S_{tar}, S_{in}, I) = - \sum_{t=1}^L \log p \left[S_{tar}^t \mid \mathcal{F}(S_{tar}^{(<t)}, S_{in}, I) \right], \quad (1)$$

where S_{tar} denotes the target sentence and L denotes the length.

Experiment

In this section, we conduct exhaustive experiments and present comprehensive analyses to evaluate the effectiveness of our proposed EAGLE. Moreover, we conduct ablation studies to verify the efficacy of each component, and we provide thorough qualitative analyses to demonstrate the superior geometric problem-solving ability of our model.

Experiment Settings

Dataset. We utilize the geometry-specific Geo170K dataset introduced by G-LLaVA (Gao et al. 2023) to train our model. Geo170K is constructed utilizing the training sets of GeoQA+ (Cao and Xiao 2022) and Geometry3K (Lu et al. 2021). Concretely, Geo170K consists of two parts: 60K examples of geometric alignment data primarily in the form of image-caption pairs, and 110K examples of geometric question-answer data with detailed CoT rationales.

Methods	Base LLM	Accuracy (%)
<i>Heuristics Baselines</i>		
Random Chance	-	25.0
Frequent	-	32.1
<i>Conventional Models</i>		
Geoformer (2022)	-	46.8
UniMath (2023)	-	50.0
<i>Multi-modal Large Language Models</i>		
LLaVA-1.5 (2024a)	Vicuna-1.5-7B	21.1
LLaVA-1.5 (2024a)	Vicuna-1.5-13B	23.2
Math-LLaVA (2024)	Vicuna-1.5-13B	48.1
G-LLaVA (2023)	LLaMA-2-7B	64.2
MAVIS (2024b)	MAMmoTH-2-7B	66.7
G-LLaVA (2023)	LLaMA-2-13B	67.0
EAGLE	Vicuna-1.5-7B	67.1

Table 1: Comparison of model performance with latest methods on the GeoQA benchmark. The best results are highlighted in bold.

Implementation Details. We develop our geometry expert model with the LLaVA-1.5 architecture (Liu et al. 2024a), which comprises a CLIP ViT-L/14 (Radford et al. 2021) as the vision encoder and the Vicuna-1.5 (Chiang et al. 2023) as the LLM backbone. We employ a two-layer MLP as the cross-modal projector to connect the visual encoder and the base LLM. The input image resolution is set to 336 by 336 pixels. In the preliminary stage, we train the vision encoder and the cross-modal projector for 1 epoch with an initial learning rate $1e^{-5}$. In the advanced stage, we integrate LoRA (Hu et al. 2022) into the vision encoder with a rank 64, and fine-tune the LLM backbone and the cross-modal projector for 2 epochs with an initial learning rate $3e^{-5}$. All experiments are conducted on 8 NVIDIA A100 GPUs, and the batch sizes is set to 6 per GPUs at both training stages.

Evaluation and Metrics. We evaluate our model on two popular multi-modal geometric benchmarks, namely GeoQA (Chen et al. 2021) and MathVista (Lu et al. 2024). GeoQA is a commonly used geometry dataset that mainly focuses on plane geometry. MathVista encompasses various mathematical tasks that require visual comprehension, where we select the Geometry Problem Solving (GPS) task within the MathVista testmini subset for evaluation. All models are assessed under a zero-shot setting, and we adopt the top-1 accuracy as the evaluation metric for all benchmarks. Our model are guided to generate responses in a fixed format after the advanced instruction tuning stage, and the predicted answers are automatically extracted via a regular expression.

Results and Analyses.

In this section, We compare the geometric reasoning ability of our EAGLE model with existing leading MLLMs, including both open-source models and closed-source models.

Comparisons on GeoQA. To evaluate the geometric reasoning capability of our model, we make comprehensive

Methods	Base LLM	Accuracy (%)
<i>Heuristics Baselines</i>		
Random Chance	-	21.6
Frequent	-	34.1
Human	-	48.4
<i>Closed-source Multi-modal Large Language Models</i>		
Genimi 1.0 Nano2 (2023)	-	23.6
Qwen-VL-Plus (2023)	Qwen-7B	38.5
Gemini 1.0 pro (2023)	-	40.4
GPT-4V (2023)	-	50.5
<i>Open-source Multi-modal Large Language Models</i>		
LLaVA-1.5 (2024a)	Vicuna-1.5-7B	17.3
LLaVA-1.5 (2024a)	Vicuna-1.5-13B	18.8
InstructBLIP (2023)	Vicuna-7B	20.7
SPHINX-V1 (2023)	LLaMA-2-13B	23.1
mPLUG-Owl (2023)	LLaMA-7B	23.6
LLaVAR (2023)	Vicuna-13B	25.0
MiniGPT4 (2024)	LLaMA-2-7B	26.0
VCAR (2024)	Vicuna-1.5-7B	34.6
Math-LLaVA-DS (2024)	Vicuna-1.5-13B	47.2
G-LLaVA (2023)	LLaMA-2-7B	53.4
G-LLaVA (2023)	LLaMA-2-13B	56.7
Math-LLaVA (2024)	Vicuna-1.5-13B	57.7
EAGLE	Vicuna-1.5-7B	54.3

Table 2: Comparison of model performance on testmini set of the MathVista benchmark for Geometry Problem Solving (GPS). Baseline results are copied from (Lu et al. 2024). The best results of closed-source and open-source MLLMs are highlighted in bold.

comparisons between EAGLE and mainstream MLLMs on GeoQA (Chen et al. 2021). As shown in Table 1, our model demonstrates superior performance among existing state-of-the-art MLLMs. Specifically, EAGLE-7B achieves 67.1% accuracy, and outperforms its baseline LLaVA-1.5-7B model by an impressive margin of 46.0%. Notably, our model employs similar model architecture and utilizes the same training dataset as G-LLaVA (Gao et al. 2023), while achieving notable 2.9% improvements compared with its 7B model. In fact, EAGLE even exceeds the G-LLaVA 13B model with only 7B trainable parameters. These improvements fully demonstrate the advancement of our visual enhancement framework in endowing our model with geometric expertise and improving its geometric reasoning capability. Moreover, our model exhibits superior performance compared with latest mathematical visual instruction tuning methods, namely Math-LLaVA (Shi et al. 2024) (trained on 360K mathematical examples) and MAVIS (Zhang et al. 2024b) (trained on more than 1.4M mathematical examples), despite being trained on a smaller dataset consisting of 170K examples. Specifically, our model outperforms Math-LLaVA-13B by 19.0% and MAVIS by 0.4%. It is noteworthy that MAVIS is a concurrent work that also focuses on visual enhancement. However, it improves the CLIP ViT separately prior to the MLLM training pipeline, which necessitates an

Methods	Preliminary Visual Enhancement	Advanced Visual Enhancement	Accuracy (%)
1	-	LoRA	63.8
2	Freeze	LoRA	62.3
3	LoRA	LoRA	65.1
4	Full Fine-tune	Full Fine-tune	64.2
5	Full Fine-tune	Freeze	66.1
EAGLE	Full Fine-tune	LoRA	67.1

Table 3: Impacts of various training strategies on vision encoder. Results are obtained on the GeoQA benchmark. In the preliminary stage, we keep the projector trainable and the LLM backbone frozen. In the advanced stage, we set both the projector and the LLM to be fully trainable.

additional laborious training procedure. In contrast, our EAGLE takes a different approach by seamlessly incorporating visual augmentation into a unified end-to-end MLLM training framework. This integration not only allows us to harness the powerful LLM for encoding geometric queries, but also provides guidance for the visual enhancement process.

Comparisons on MathVista. We additionally compare our model with leading MLLMs on the testmini split of the MathVista (Lu et al. 2024) benchmark. As shown in Table 2, our EAGLE achieves 54.3% accuracy in Geometry Problem Solving and surpasses GPT-4V by 3.8%. Compared with other 7B models, EAGLE also exhibits superior performance. For example, EAGLE exceeds its baseline model LLaVA-1.5-7B with a clear margin of 37.0%. Moreover, our model also outperforms Math-LLaVA-DS by 7.1%, which is a 13B model trained with 40K high-quality images and question-answer pairs. These improvements demonstrate the superiority of enhancing the vision encoder in an end-to-end MLLM training framework, aided by the dynamic LLM backbone. This approach effectively directs our model to focus on nuanced geometric clues and acquire high-level geometric reasoning capabilities.

Ablation Study

To demonstrate the efficacy of our training framework, we compare EAGLE with a series of variants in Table 3.

Different Preliminary Visual Enhancement Strategies.

We first verify the necessity to conduct the preliminary visual enhancement. Comparing Method 1 and our EAGLE, we observe that the model trained without the preliminary visual enhancement lags behind EAGLE by 3.3%. This observation empirically supports our hypothesis that MLLMs necessitate exposure to sufficient geometric figures and the acquisition of fundamental geometric knowledge to bridge the inherent domain gap, thereby establishing the groundwork for subsequent geometric reasoning.

Based on above observation, we further delve into the optimal visual enhancement strategy. Comparing EAGLE with Method 2 and Method 3, it is clear that fine-tuning the entire vision encoder in the preliminary stage leads to superior results. We contend that despite being trained on a

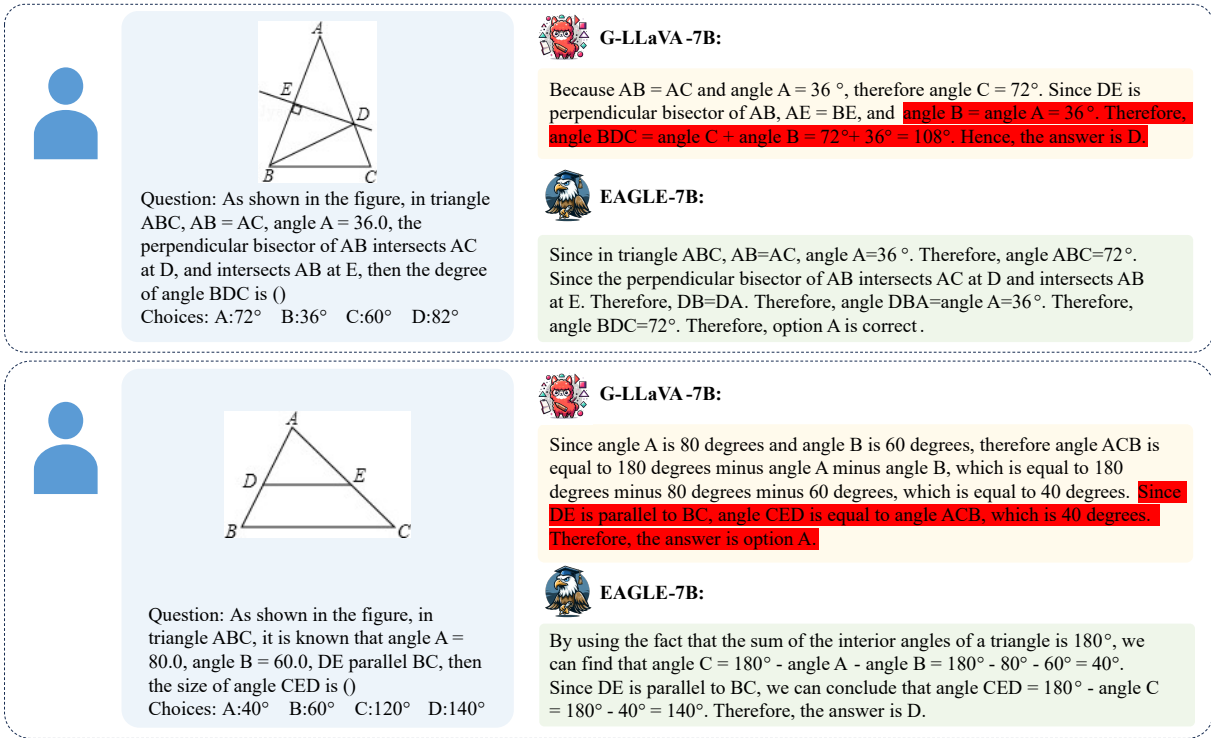


Figure 4: Demonstration of the geometric problem-solving capability by G-LLaVA (Gao et al. 2023) and our EAGLE.

large corpus of natural images, the CLIP ViT lacks exposure to sufficient geometry diagrams, thus impeding its performance in geometric perception. Therefore, fully fine-tuning ViT could effectively facilitate the visual augmentation process. Moreover, we observe that Method 2 exhibits inferior performance compared with Method 1, which highlights the importance of optimizing the cross-modal projector with geometric image-caption pairs. Otherwise, the projector may experience unsatisfactory visual-linguistic alignments that hinder MLLMs’ problem solving capabilities.

Different Advanced Visual Enhancement Strategies.

As the cognitive core of MLLMs, the base LLM is usually optimized to acquire the mathematical problem-solving competence during the instruction tuning process. Given its strength, We wonder whether elevating the vision encoder and the LLM backbone simultaneously could lead to a more advanced geometric expert. Therefore, we conduct several ablation experiments for exploration. As shown in Table 3, Methods 4, 5 and our EAGLE employ different visual fine-tuning strategies in the advanced visual enhancement stage. We observe that incorporating LoRA modules into the vision encoder achieves the best performance, while fully fine-tuning the vision encoder results in inferior results, even poorer than keeping the visual backbone frozen. A plausible explanation is that the vision encoder has gained fundamental geometric knowledge from the image-caption data during the preliminary stage. As a result, a slight fine-tuning process further enhances its visual comprehension capabilities and promotes superior performance. Conversely, fully

Methods	LLM Optimization	Accuracy (%)
LLaVA-1.5-7B	-	21.1
EAGLE*	Freeze	31.4
EAGLE	Full Fine-tune	67.1

Table 4: Impact of the core LLM during the advanced visual enhancement stage. EAGLE* denotes the variant model with a frozen LLM. Results are obtained on the GeoQA benchmark.

fine-tuning the entire ViT may disrupt its inherent knowledge structure and result in catastrophic forgetting.

Impacts of the LLM backbone. To explore the role of the LLM backbone in addressing multi-modal geometric reasoning problems, we attempt to freeze the LLM backbone during the whole training process, while the rest modules (the vision encoder and the projector) still follow the optimal training strategy discovered in previous experiments. As shown in Table 4, freezing the LLM backbone results in huge performance drops, which falls behind our EAGLE by 35.7%. This observation demonstrates the fundamental effect of the LLM backbone in solving geometric problems with visual contexts. Interestingly, we observe that this comparative variant achieves 10.3% improvements compared with the baseline LLaVA-1.5 model. Given that the only difference between them lies in the geometric augmentation of the vision encoder and the cross-modal projector, this result further verifies the significant role of our proposed visual

enhancement strategy.

Qualitative Analysis

In Figure 4, we compare the geometric problem-solving performance of EAGLE with the representative geometric model G-LLaVA (Gao et al. 2023). Our model displays superior visual perception proficiency and strong geometric reasoning capability, which accurately captures key geometric elements and provides reliable CoT solutions. In contrast, G-LLaVA (Gao et al. 2023) suffers from errors in effectively utilizing geometric principles, leading to incorrect answers.

Potential for Broader Application

Our proposed end-to-end visual enhancement framework is not specified in geometric problem solving. Actually, it has the potential to boost the performance of MLLMs for various multi-modal tasks. Therefore, we propose several potential applications of our LLM-empowered visual instruction tuning framework for further inspirations, as outlined below.

- Besides geometric elements, the CLIP ViT also displays unsatisfactory perception performance facing other mathematical-related scenarios, such as tables and functions. This visual inadequacy severely limits MLLMs’ problem-solving capabilities. Therefore, unlocking the vision encoder and tailoring it to specific scenarios seems to be a promising paradigm to enhance the performance of advanced MLLMs.
- Our EAGLE highlights the possibility to enhance the vision encoder through robust LLMs. Hence, harnessing their advanced linguistic encoding capabilities is promising for various cross-modal tasks. For example, a segmentation model could perform better by integrating a LLM text encoder to interpret intricate prompts.
- Our experiments demonstrate the effectiveness of the LLM-empowered visual enhancement framework. Consequently, we contemplate the efficacy of leveraging generative LLMs for cross-modal alignments. For example, rather than employing contrastive learning to train CLIP with image-text pairs, we can input image features extracted by a raw ViT into LLMs for text generation. Subsequently, the ViT undergoes iterative enhancements by optimizing the alignment between generated sentences and real captions. We leave the corresponding studies for future work.

Related Work

Multi-modal Large Language Models

Recent years have witnessed thriving developments for large language models (Touvron et al. 2023a; Bai et al. 2022; Touvron et al. 2023b), which displays remarkable performance across various tasks. Concurrently, many researchers attempt to harness the prowess of LLMs in diverse multi-modal scenarios, leading to the prosperity of multi-modal large language models (OpenAI 2023; Liu et al. 2024b; Ye et al. 2024). Modern MLLMs typically comprise a vision encoder that extracts visual clues (e.g. CLIP (Radford et al.

2021)), a cross-modal projector that aligns visual and textual features, and a language foundation model that serves as the cognitive core (e.g. LLaMA (Touvron et al. 2023a)). In early studies, MLLMs primarily focus on conventional vision-language tasks, as demonstrated BLIP-2 (Li et al. 2023) and Mini-GPT4 (Zhu et al. 2024). Recently, in light of the remarkable advancements achieved by LLMs in complex reasoning (Yu, He, and Ying 2024; Yuan et al. 2024), there has been a surge of research focusing on multi-modal reasoning (Wang et al. 2024a,b). For example, Zheng *et al.* (Zheng et al. 2023) devised a novel DDCoT prompting technique that decouples LLMs’ reasoning and recognition capabilities, enabling the transfer of these advancements to multi-modal contexts. He *et al.* (He et al. 2024) proposed to improve the multi-modal CoT capability through latent space learning. Despite these significant achievements, we observe that MLLMs still face challenges in effectively addressing multi-modal mathematical problems involving geometric elements.

Geometric Reasoning

Geometric reasoning is a challenging multi-modal mathematical reasoning problem, which requires MLLMs to possess the proficiency in both visual perception and mathematical reasoning. Several geometric datasets have been introduced to promote the advancement of geometric reasoning, such as Geometry3K (Lu et al. 2021), GeoQA (Chen et al. 2021), and GeoQA+ (Cao and Xiao 2022). As a representative work, Gao *et al.* (Gao et al. 2023) constructed a multi-modal geometry dataset Geo170K, and subsequently developed a competitive geometric MLLM model named G-LLaVA. Shi *et al.* (Shi et al. 2024) presented Math-LLaVA, a multi-modal mathematical MLLM trained on curated MathV360K dataset. These studies mainly focus on enhancing the geometric reasoning strength, while neglecting the enhancement of visual proficiency. Recently, researchers have noticed this barrier and made some inspiring endeavors. For example, VCAR (Jia et al. 2024) incorporated a visual description generation task into the MLLM training process to enhance visual understandings. MAVIS (Zhang et al. 2024b) developed a math-specific vision encoder with the curated MAVIS-Caption dataset and employed a mathematics-enhanced LLM MAMmoTH-2 (Yue et al. 2024) as the LLM backbone. However, these studies mostly consider visual augmentation as a separate training step, which is inconsistent with the subsequent LLM fine-tuning. In contrast, we propose a novel end-to-end MLLM framework with LLM-empowered visual instruction tuning, which harnesses the strength of powerful LLMs to facilitate visual enhancement.

Conclusion

In this paper, we focus on mitigating the visual deficiency of current MLLMs in solving geometric problems. To achieve this, We propose a novel two-stage end-to-end framework named EAGLE, which elevates geometric reasoning through LLM-empowered visual instructing tuning. Our approach leverages the strength of LLMs in both stages to boost visual

comprehension. Specifically, our model acquires basic geometric knowledge in the preliminary stage and explores subtle geometric clues in the advanced stage. EAGLE achieves leading performance on popular multi-modal mathematical geometric benchmarks, revealing the significant potential of utilizing LLMs to improve the visual proficiency. We hope our work could contribute innovative insights to the MLLM literature and promote the advancement of the visual perception capabilities within MLLMs.

References

- Abnar, S.; and Zuidema, W. 2020. Quantifying attention flow in transformers. In *Proceedings of the 58th Annual Meeting of the Association for Computational Linguistics*, 4190–4197.
- Antol, S.; Agrawal, A.; Lu, J.; Mitchell, M.; Batra, D.; Zitnick, C. L.; and Parikh, D. 2015. Vqa: Visual question answering. In *Proceedings of the IEEE International Conference on Computer Vision*, 2425–2433.
- Bai, J.; Bai, S.; Yang, S.; Wang, S.; Tan, S.; Wang, P.; Lin, J.; Zhou, C.; and Zhou, J. 2023. Qwen-vl: A frontier large vision-language model with versatile abilities. *arXiv preprint arXiv:2308.12966*.
- Bai, Y.; Jones, A.; Ndousse, K.; Askell, A.; Chen, A.; Das-Sarma, N.; Drain, D.; Fort, S.; Ganguli, D.; Henighan, T.; et al. 2022. Training a helpful and harmless assistant with reinforcement learning from human feedback. *arXiv preprint arXiv:2204.05862*.
- Cao, J.; and Xiao, J. 2022. An augmented benchmark dataset for geometric question answering through dual parallel text encoding. In *Proceedings of the 29th International Conference on Computational Linguistics*, 1511–1520.
- Chai, L.; Yang, J.; Sun, T.; Guo, H.; Liu, J.; Wang, B.; Liang, X.; Bai, J.; Li, T.; Peng, Q.; et al. 2024. xcot: Cross-lingual instruction tuning for cross-lingual chain-of-thought reasoning. *arXiv preprint arXiv:2401.07037*.
- Chen, J.; Li, T.; Qin, J.; Lu, P.; Lin, L.; Chen, C.; and Liang, X. 2022. Unigeo: Unifying geometry logical reasoning via reformulating mathematical expression. In *Proceedings of the 2022 Conference on Empirical Methods in Natural Language Processing*, 3313–3323.
- Chen, J.; Tang, J.; Qin, J.; Liang, X.; Liu, L.; Xing, E.; and Lin, L. 2021. GeoQA: A Geometric Question Answering Benchmark Towards Multimodal Numerical Reasoning. In *Findings of the Association for Computational Linguistics: ACLI-JCNLP 2021*, 513–523.
- Chiang, W.-L.; Li, Z.; Lin, Z.; Sheng, Y.; Wu, Z.; Zhang, H.; Zheng, L.; Zhuang, S.; Zhuang, Y.; Gonzalez, J. E.; et al. 2023. Vicuna: An open-source chatbot impressing gpt-4 with 90%* chatgpt quality. <https://lmsys.org/blog/2023-03-30-vicuna>.
- Dai, W.; Li, J.; Li, D.; Tiong, A.; Zhao, J.; Wang, W.; Li, B.; Fung, P.; and Hoi, S. 2023. InstructBLIP: Towards General-purpose Vision-Language Models with Instruction Tuning. In *Thirty-seventh Conference on Neural Information Processing Systems*.
- Gao, J.; Pi, R.; Zhang, J.; Ye, J.; Zhong, W.; Wang, Y.; Hong, L.; Han, J.; Xu, H.; Li, Z.; et al. 2023. G-llava: Solving geometric problem with multi-modal large language model. *arXiv preprint arXiv:2312.11370*.
- He, L.; Li, Z.; Cai, X.; and Wang, P. 2024. Multi-modal latent space learning for chain-of-thought reasoning in language models. In *Proceedings of the AAAI Conference on Artificial Intelligence*, volume 38, 18180–18187.
- Hu, E. J.; yelong shen; Wallis, P.; Allen-Zhu, Z.; Li, Y.; Wang, S.; Wang, L.; and Chen, W. 2022. LoRA: Low-Rank Adaptation of Large Language Models. In *The Tenth International Conference on Learning Representations*.
- Imani, S.; Du, L.; and Shrivastava, H. 2023. Mathprompter: Mathematical reasoning using large language models. *arXiv preprint arXiv:2303.05398*.
- Ji, Z.; Li, Z.; Zhang, Y.; Wang, H.; Pang, Y.; and Li, X. 2024. Hierarchical matching and reasoning for multi-query image retrieval. *Neural Networks*, 173: 106200.
- Jia, M.; Zhang, Z.; Yu, W.; Jiao, F.; and Jiang, M. 2024. Describe-then-Reason: Improving Multimodal Mathematical Reasoning through Visual Comprehension Training. *arXiv preprint arXiv:2404.14604*.
- Li, J.; Li, D.; Savarese, S.; and Hoi, S. 2023. Blip-2: Bootstrapping language-image pre-training with frozen image encoders and large language models. In *International Conference on Machine Learning*, 19730–19742.
- Liang, Z.; Yang, T.; Zhang, J.; and Zhang, X. 2023. Unimath: A foundational and multimodal mathematical reasoner. In *Proceedings of the 2023 Conference on Empirical Methods in Natural Language Processing*, 7126–7133.
- Lin, Z.; Liu, C.; Zhang, R.; Gao, P.; Qiu, L.; Xiao, H.; Qiu, H.; Lin, C.; Shao, W.; Chen, K.; et al. 2023. Sphinx: The joint mixing of weights, tasks, and visual embeddings for multi-modal large language models. *arXiv preprint arXiv:2311.07575*.
- Liu, H.; Li, C.; Li, Y.; and Lee, Y. J. 2024a. Improved baselines with visual instruction tuning. In *Proceedings of the IEEE/CVF Conference on Computer Vision and Pattern Recognition*, 26296–26306.
- Liu, H.; Li, C.; Wu, Q.; and Lee, Y. J. 2024b. Visual instruction tuning. *Advances in Neural Information Processing Systems*, 36.
- Lu, P.; Bansal, H.; Xia, T.; Liu, J.; Li, C.; Hajishirzi, H.; Cheng, H.; Chang, K.-W.; Galley, M.; and Gao, J. 2024. MathVista: Evaluating Mathematical Reasoning of Foundation Models in Visual Contexts. In *The Twelfth International Conference on Learning Representations*.
- Lu, P.; Gong, R.; Jiang, S.; Qiu, L.; Huang, S.; Liang, X.; and Zhu, S.-C. 2021. Inter-GPS: Interpretable Geometry Problem Solving with Formal Language and Symbolic Reasoning. In *Proceedings of the 59th Annual Meeting of the Association for Computational Linguistics*, 6774–6786.
- OpenAI. 2023. GPT-4V(ision).
- Radford, A.; Kim, J. W.; Hallacy, C.; Ramesh, A.; Goh, G.; Agarwal, S.; Sastry, G.; Askell, A.; Mishkin, P.; Clark, J.;

- et al. 2021. Learning transferable visual models from natural language supervision. In *International Conference on Machine Learning*, 8748–8763.
- Shi, W.; Hu, Z.; Bin, Y.; Liu, J.; Yang, Y.; Ng, S.-K.; Bing, L.; and Lee, R. K.-W. 2024. Math-LLaVA: Bootstrapping Mathematical Reasoning for Multimodal Large Language Models. *arXiv preprint arXiv:2406.17294*.
- Sun, T.; Chai, L.; Yang, J.; Yin, Y.; Guo, H.; Liu, J.; Wang, B.; Yang, L.; and Li, Z. 2024. Unicoder: Scaling code large language model via universal code. In *Proceedings of the 62nd Annual Meeting of the Association for Computational Linguistics*.
- Team, G.; Anil, R.; Borgeaud, S.; Wu, Y.; Alayrac, J.-B.; Yu, J.; Soricut, R.; Schalkwyk, J.; Dai, A. M.; Hauth, A.; et al. 2023. Gemini: a family of highly capable multimodal models. *arXiv preprint arXiv:2312.11805*.
- Touvron, H.; Lavril, T.; Izacard, G.; Martinet, X.; Lachaux, M.-A.; Lacroix, T.; Rozière, B.; Goyal, N.; Hambro, E.; Azhar, F.; et al. 2023a. Llama: Open and efficient foundation language models. *arXiv preprint arXiv:2302.13971*.
- Touvron, H.; Martin, L.; Stone, K.; Albert, P.; Almahairi, A.; Babaei, Y.; Bashlykov, N.; Batra, S.; Bhargava, P.; Bhosale, S.; et al. 2023b. Llama 2: Open foundation and fine-tuned chat models. *arXiv preprint arXiv:2307.09288*.
- Wang, Y.; Chen, W.; Han, X.; Lin, X.; Zhao, H.; Liu, Y.; Zhai, B.; Yuan, J.; You, Q.; and Yang, H. 2024a. Exploring the reasoning abilities of multimodal large language models (mllms): A comprehensive survey on emerging trends in multimodal reasoning. *arXiv preprint arXiv:2401.06805*.
- Wang, Z.; Han, Z.; Chen, S.; Xue, F.; Ding, Z.; Xiao, X.; Tresp, V.; Torr, P.; and Gu, J. 2024b. Stop reasoning! when multimodal llms with chain-of-thought reasoning meets adversarial images. *arXiv preprint arXiv:2402.14899*.
- Xu, K.; Ba, J.; Kiros, R.; Cho, K.; Courville, A.; Salakhudinov, R.; Zemel, R.; and Bengio, Y. 2015. Show, attend and tell: Neural image caption generation with visual attention. In *International Conference on Machine Learning*, 2048–2057.
- Ye, Q.; Xu, H.; Xu, G.; Ye, J.; Yan, M.; Zhou, Y.; Wang, J.; Hu, A.; Shi, P.; Shi, Y.; et al. 2023. mplug-owl: Modularization empowers large language models with multimodality. *arXiv preprint arXiv:2304.14178*.
- Ye, Q.; Xu, H.; Ye, J.; Yan, M.; Hu, A.; Liu, H.; Qian, Q.; Zhang, J.; and Huang, F. 2024. mplug-owl2: Revolutionizing multi-modal large language model with modality collaboration. In *Proceedings of the IEEE/CVF Conference on Computer Vision and Pattern Recognition*, 13040–13051.
- Yu, J.; He, R.; and Ying, Z. 2024. Thought Propagation: An Analogical Approach to Complex Reasoning with Large Language Models. In *The Twelfth International Conference on Learning Representations*.
- Yuan, L.; Cui, G.; Wang, H.; Ding, N.; Wang, X.; Deng, J.; Shan, B.; Chen, H.; Xie, R.; Lin, Y.; et al. 2024. Advancing llm reasoning generalists with preference trees. *arXiv preprint arXiv:2404.02078*.
- Yue, X.; Zheng, T.; Zhang, G.; and Chen, W. 2024. Mammoth2: Scaling instructions from the web. *arXiv preprint arXiv:2405.03548*.
- Zhang, D.; Yu, Y.; Li, C.; Dong, J.; Su, D.; Chu, C.; and Yu, D. 2024a. Mm-llms: Recent advances in multimodal large language models. *arXiv preprint arXiv:2401.13601*.
- Zhang, R.; Wei, X.; Jiang, D.; Zhang, Y.; Guo, Z.; Tong, C.; Liu, J.; Zhou, A.; Wei, B.; Zhang, S.; et al. 2024b. MAVIS: Mathematical Visual Instruction Tuning. *arXiv preprint arXiv:2407.08739*.
- Zhang, Y.; Zhang, R.; Gu, J.; Zhou, Y.; Lipka, N.; Yang, D.; and Sun, T. 2023. Lllavar: Enhanced visual instruction tuning for text-rich image understanding. *arXiv preprint arXiv:2306.17107*.
- Zheng, G.; Yang, B.; Tang, J.; Zhou, H.-Y.; and Yang, S. 2023. Ddcot: Duty-distinct chain-of-thought prompting for multimodal reasoning in language models. *Advances in Neural Information Processing Systems*, 36: 5168–5191.
- Zhu, D.; Chen, J.; Shen, X.; Li, X.; and Elhoseiny, M. 2024. MiniGPT-4: Enhancing Vision-Language Understanding with Advanced Large Language Models. In *The Twelfth International Conference on Learning Representations*.

Appendix Overview

This appendix for **EAGLE**: Elevating Geometric Reasoning through LLM-empowered Visual Instruction Tuning is organized as follows: 1) additional geometric attention map visualizations of the CLIP ViT and the geometry-augmented vision encoder of our EAGLE. 2) detailed training configurations. 3) in-depth analysis of the preliminary stage. 4) further qualitative studies on GeoQA (Chen et al. 2021) and MathVista (Lu et al. 2024).

1.A Additional Visualization Illustrations

We conduct more attention map visualizations to demonstrate the visual perception deficiencies of the widely adopted CLIP ViT (Radford et al. 2021). As illustrated in Figure 5, various examples indicate that CLIP ViT struggles to capture key geometric elements within diagrams. In contrast, after the two-stage LLM-empowered visual enhancement, our EAGLE accurately perceives geometric elements, including points, lines, and angles. Consequently, EAGLE can perform precise problem-solving processes with reliable visual perceptions.

1.B Training Details

We present the detailed training hyper-parameter settings of EAGLE during the two visual enhancement stages, as shown in Table 5.

1.C Further Analysis of the Preliminary Stage

In our proposed framework, the preliminary stage utilizes geometric image-caption pairs to provide the MLLM with basic geometric knowledge, laying the groundwork for subsequent geometric reasoning enhancement. To thoroughly verify the necessity of the preliminary stage, we remove it from the training pipeline, focusing solely on the advanced stage with question-answer pairs. Additionally, we explore various visual fine-tuning strategies during the advanced stage to conduct comprehensive studies, as shown in Table 6. Notably, despite applying various visual fine-tuning strategies, models trained without the preliminary stage (Methods 1 to 3) underperform our EAGLE by more than 2.5%. These results clearly demonstrate the effectiveness of the preliminary visual enhancement stage with a frozen LLM backbone. Furthermore, although Methods 1 to 3 omit the preliminary stage, they perform comparably to, or even surpass, the G-LLaVA 7B model (Gao et al. 2023), which utilizes the same Geo170K (Gao et al. 2023) dataset. A plausible explanation is that G-LLaVA freezes the vision encoder throughout the entire training process, which prevents its vision encoder from acquiring geometric knowledge from geometric image-caption data. This comparison further validates the necessity and effectiveness of our proposed visual enhancement framework.

1.D Qualitative Studies

In this section, we present comprehensive geometric reasoning cases to demonstrate the geometric problem-solving capabilities of our EAGLE.

Methods	Preliminary Visual Enhancement	Advanced Visual Enhancement
Batch Size		48
Learning Rate (LR)	1e-5	3e-5
LR Schedule		cosine decay
LR Warmup Ratio		0.03
Weight Decay		0
Epoch	1	2
Optimizer		AdamW
LoRA Alpha	-	16
LoRA Rank	-	64
LoRA Dropout	-	0.05

Table 5: Hyper-parameter settings

Methods	Preliminary Visual Enhancement	Advanced Visual Enhancement	Accuracy (%)
1	-	LoRA	63.8
2	-	Full Fine-tune	64.3
3	-	Freeze	64.6
G-LLaVA-7B (2023)	Freeze	Freeze	64.2
EAGLE-7B	Full Fine-tune	LoRA	67.1

Table 6: Further analysis of the necessity of preliminary stage with various training strategies on the vision encoder. Results are obtained on the GeoQA benchmark. When the preliminary stage is included, the projector is kept trainable while the LLM backbone is frozen. For the advanced stage, both the projector and the LLM backbone are fully trainable.

Case Studies on GeoQA We first conduct case studies on GeoQA (Chen et al. 2021). As illustrated in Figure 6, our EAGLE not only accurately interprets geometric diagrams, but also provides correct answers along with detailed CoT rationales. Specifically, EAGLE exhibits reliable visual perception proficiency. In Figure 6 (a), EAGLE correctly distinguishes between angle 1 and angle 2, and identifies the relationship between angle a and angle BEF, which is not explicitly mentioned in the textual questions. Moreover, EAGLE showcases its ability to apply geometric knowledge effectively. For instance, in Figure 6 (b), EAGLE accurately utilizes the inscribed angle theorem to determine that angle C is half of angle BOA.

Case Studies on MathVista We also provide additional reasoning cases from the testmini set of MathVista (Lu et al. 2024) for Geometry Problem Solving (GPS). As shown in Figure 7, EAGLE effectively addresses geometric problems in various types, including calculations of area, angle, trigonometric functions, and length. Notably, in Figure 7 (a), EAGLE even demonstrates the ability to draw auxiliary lines to aid in problem solving, such as connecting AO and CO to form triangle OAC. These resolution processes further highlight the robust problem-solving capabilities of our proposed model.

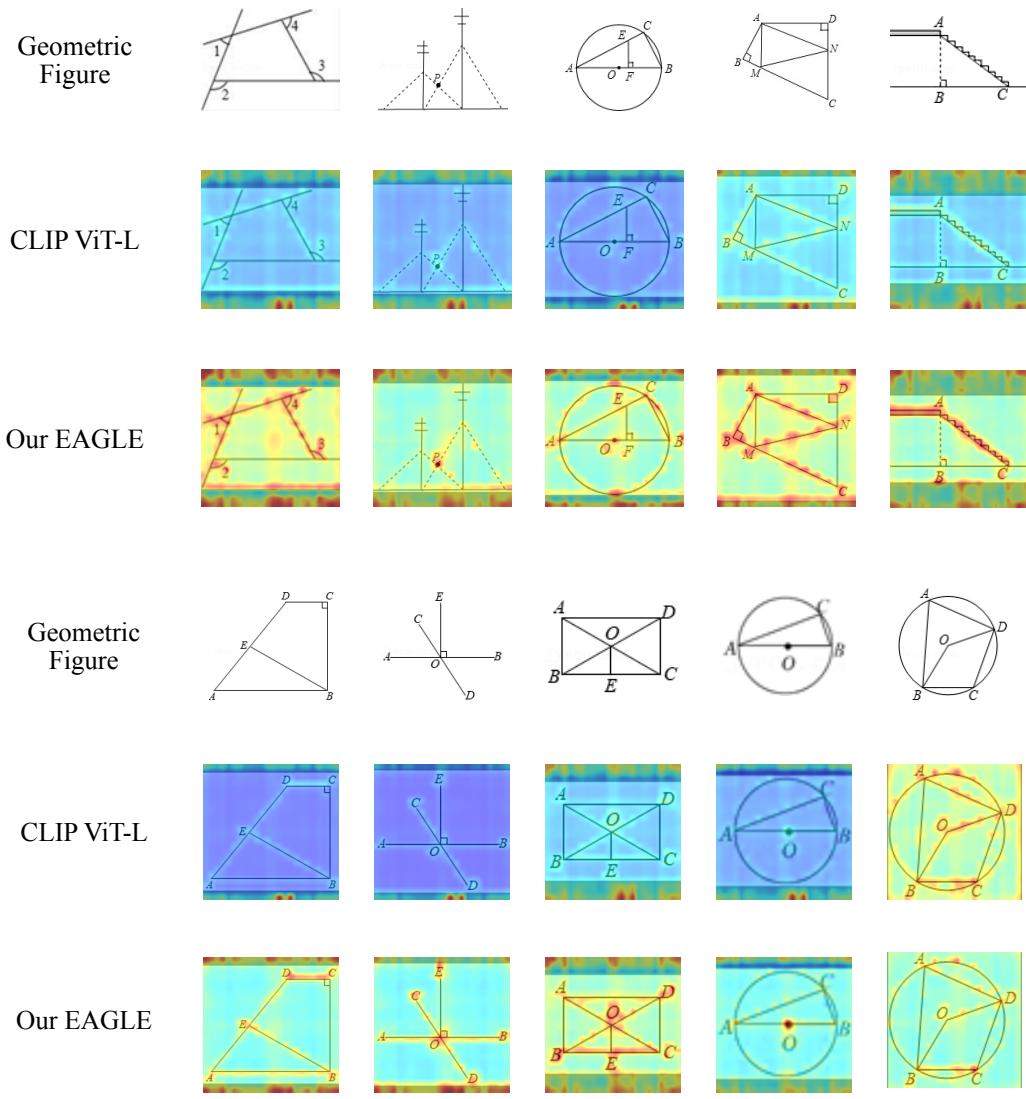


Figure 5: Comparison of attention maps between CLIP ViT (Radford et al. 2021) and our EAGLE.

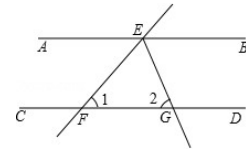


Question: As shown in the figure, AB parallel CD, straight line EF intersects AB at point E, intersects CD at point F, EG bisects angle BEF, and it intersects CD at point G, angle 1 = 50.0, then angle 2 is equal to ()
Choices: A:50° B:60° C:65° D:90°



Solution: Since AB is parallel to CD, we have the following relationships: angle 1 + angle BEF = 180°, angle 1 = 50°, angle BEF = 130°. Also, since EG bisects angle BEF, we have angle BEG = 1/2 angle BEF = 65°. Therefore, angle 2 = angle BEG = 65°. Thus, option C is the correct answer.

(a)

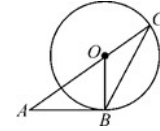


Question: As shown in the figure, AB is tangent to circle O at point B, and the extended line of AO intersects circle O at point C. Connect BC, if angle A = 36.0, then angle C is equal to ()
Choices: A:36° B:54° C:60° D:27°



Solution: Since AB is tangent to circle O at point B, therefore, angle ABO = 90°. Since angle A = 36°, therefore, angle BOA = 54°. Therefore, according to the inscribed angle theorem, angle C = 1/2 angle BOA = 27°. Therefore, the correct choice is D.

(b)

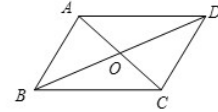


Question: In parallelogram ABCD, the diagonal AC and BD intersect at point O, angle DAC = 42.0, angle CBD = 23.0, then angle COD is ().
Choices: A:61° B:63° C:65° D:67°



Solution: Since quadrilateral ABCD is a parallelogram, we have AD parallel to BC. Therefore, angle BCA is equal to angle DAC, which is 42 degrees. Angle COD can be calculated as the sum of angle CBD and angle BCA, which is 42 degrees plus 23 degrees, equal to 65 degrees. Therefore, the correct answer is C.

(c)



Question: As shown in the figure, in circle O, chord AC parallel radius OB, angle BOC = 50.0, then the degree of angle OAB is ()
Choices: A:25° B:50° C:60° D:30°



Solution: Since AC is parallel to OB, therefore angle BOC is equal to angle ACO which is 50 degrees. Also, OA is equal to OC, so angle OAC is equal to angle ACO which is 50 degrees. Since angle CAB is half of angle BOC, it is 25 degrees. Therefore, angle BAO is equal to angle OAC minus angle CAB which is 50 degrees minus 25 degrees which is 25 degrees. Hence, option A is selected.

(d)

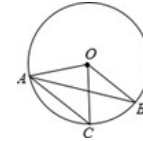


Figure 6: Geometric reasoning cases of our proposed EAGLE on the GeoQA benchmark.

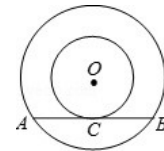


Question: As shown in the figure, in the two concentric circles, the chord AB of the great circle is tangent to the small circle at point C. If AB = 6.0, the area of the ring is ()
Choices: A:9π B:6π C:3π D:π



Solution: Connect OA and OC as shown in the figure. Since the chord AB of the larger circle is tangent to the smaller circle at point C, we have OC perpendicular to AB. Therefore, AC=BC=1/2AB=3. In right triangle OAC, OA²-OC²=AC²=3²=9. Thus, the area of the annulus in the figure is S_{larger circle} - S_{smaller circle} = π·OA² - π·OC² = π(OA² - OC²) = 9π. Therefore, the answer is A.

(a)

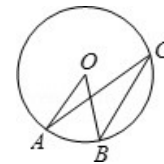


Question: As shown in the figure, point O is the center of ⊙ O, points A, B, and C are on ⊙ O, AO ∥ BC, ∠AOB = 40.0, then the degree of ∠OAC is equal to ()
Choices: A:40° B:60° C:50° D:20°



Solution: Since AO is parallel to BC, we have angle OAC = angle ACB. Additionally, both angle AOB and angle ACB are angles that are opposite to arc AB. Therefore, angle ACB = 1/2 angle AOB = 20°. Hence, the measure of angle OAC is 20°. Therefore, the answer is D.

(b)



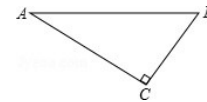
Question: As shown in the figure: In △ABC, ∠C = 90.0, AC = 8.0, AB = 10.0, then the value of sin B is equal to ()



Choices: A:3/5 B:4/5 C:3/4 D:4/3

Solution: Since in right triangle ABC, angle C = 90°, AC = 8, AB = 10, therefore sin B = AC/AB = 8/10 = 4/5. Thus, the answer is B.

(c)



Question: As shown in the figure, in the diamond ABCD, two diagonal lines AC = 12.0, BD = 16.0, then the edge length of this diamond is ()
Choices: A:10 B:8 C:6 D:5



Solution: Since the diagonals of a rhombus are perpendicular bisectors of each other, triangle AOB is a right-angled triangle. Also, we know that AC is equal to 2 times AO and BD is equal to 2 times BO. Therefore, AO is equal to 6 and BO is equal to 8. Consequently, AB can be found using the Pythagorean theorem, which gives us √(AO² + BO²) = 10. Therefore, the correct answer is option A.

(d)

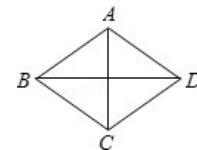


Figure 7: Geometric reasoning cases of our proposed EAGLE on the MathVista benchmark.